

RESEARCH ARTICLE

A microRNA-clinical prognosis model to predict the overall survival for kidney renal clear cell carcinoma

Yating Zhan¹ | Rongrong Zhang¹ | Chunxue Li¹ | Xuantong Xu¹ | Kai Zhu¹ | Zhan Yang¹ | Jianjian Zheng¹ | Yong Guo² 

¹Key Laboratory of Diagnosis and Treatment of Severe Hepato-Pancreatic Diseases of Zhejiang Province, The First Affiliated Hospital of Wenzhou Medical University, Wenzhou, China

²Department of Urology, The First Affiliated Hospital of Wenzhou Medical University, Wenzhou, China

Correspondence

Yong Guo, Department of Urology, The First Affiliated Hospital of Wenzhou Medical University, No. 2 Fuxue lane, Wenzhou, Zhejiang, P.R. China.
Email: guoyong@wmu.edu.cn

Jianjian Zheng, Key Laboratory of Diagnosis and Treatment of Severe Hepato-Pancreatic Diseases of Zhejiang Province, The First Affiliated Hospital of Wenzhou Medical University, No.2 Fuxue lane, Wenzhou, Zhejiang, P.R. China
Email: 120378196@qq.com

Funding information

National Natural Science Foundation of China, Grant/Award Number: 81873576; Medical Health Science and Technology Project of Zhejiang Provincial Health Commission, Grant/Award Number: 2020RC081; Wenzhou Medical University Basic Scientific Research, Grant/Award Number: KYYW201904

Abstract

Numerous studies have shown that microRNA (miRNA) serves as key regulatory factors in the origin and development of cancers. However, the biological mechanisms of miRNAs in kidney renal clear cell carcinoma (KIRC) are still unknown. It is necessary to construct an effective miRNA-clinical model to predict the prognosis of KIRC. In this study, 94 differentially expressed miRNAs were found between para-tumor and tumor tissues based on the Cancer Genome Atlas (TCGA) database. Seven miRNAs (hsa-miR-21-5p, hsa-miR-3613-5p, hsa-miR-144-5p, hsa-miR-376a-5p, hsa-miR-5588-3p, hsa-miR-1269a, and hsa-miR-137-3p) were selected as prognostic indicators. According to their cox coefficient, a risk score formula was constructed. Patients with risk scores were divided into high- and low-risk groups based on the median score. Kaplan–Meier curves analysis showed that the low-risk group had a better survival probability compared to the high-risk group. The area under the ROC curve (AUC) value of the miRNA model was 0.744. In comparison with clinical features, the miRNA model risk score was considered as an independent prognosis factor in multivariate Cox regression analysis. In addition, we built a nomogram including age, metastasis, and miRNA prognostic model based on the results of multivariate Cox regression analysis. The decision curve analysis (DCA) revealed the clinical net benefit of the prognostic model. Gene set enrichment analysis (GSEA) results suggested that several important pathways may be the potential pathways for KIRC. The results of Gene Ontology (GO) and Kyoto Encyclopedia of Genes and Genomes (KEGG) enrichment analysis for the target genes of 7 miRNAs revealed that miRNAs may participate in KIRC progression via many specific pathways. Additionally, the levels of seven prognostic miRNAs showed a significant difference between KIRC tissues and adjacent non-tumorous tissues. In conclusion, the miRNA-clinical model provides an effective and accurate way to predict the prognosis of KIRC.

KEY WORDS

kidney renal clear cell carcinoma, microRNA, nomogram, prognosis model

Yating Zhan, Rongrong Zhang, and Chunxue Li have contributed equally to this work.

This is an open access article under the terms of the Creative Commons Attribution License, which permits use, distribution and reproduction in any medium, provided the original work is properly cited.

© 2021 The Authors. *Cancer Medicine* published by John Wiley & Sons Ltd.

1 | INTRODUCTION

Renal cell carcinoma (RCC) is known as one of the most common cancers throughout the world. Generally, RCC is divided into three types: kidney renal clear cell carcinoma (KIRC), kidney renal papillary cell carcinoma (KIRP), and malignancies of the chromophobe.¹ Among them, KIRC is the most common type of kidney cell cancers and accounts for approximately 80–90% of RCC.^{2,3} In most cases, KIRC is resistant to radiotherapy and chemotherapy, and the main treatment is surgery.⁴ Despite early surgical treatment is taken, 30% of patients are at a relatively higher risk of developing metastasis and recurrence.⁵ Therefore, KIRC still threatens human health and life as a malignant disease. Until now, the roles of miRNAs (miRNAs) in KIRC are still largely unknown and few crucial biomarkers have been found. Therefore, it is necessary to explore effective biomarkers for the prognosis of KIRC.

MiRNAs, consisting of 21–23 nucleotides, are evolutionarily conserved single-strand endogenous noncoded RNAs that widely exist in humans and animals.⁶ MiRNAs are generally not translated into proteins, but they are closely associated with the complex cell mechanisms responsible for gene expression. In addition, miRNAs play a crucial role in various human cancers.⁷ For example, miR-21 could influence the invasiveness and angiogenesis of renal cell carcinoma cells by the PDCD4/c-Jun (AP-1) signaling pathway.⁸ Feng et al. revealed that circRNA_001287 promotes the proliferation of renal cell carcinoma through miR-144/CEP55 signaling pathway.⁹

In this study, we aimed to construct a novel prognostic model including miRNA signature and clinical factors. Mature miRNA sequencing data and the corresponding clinical information of KIRC were downloaded from the Cancer Genome Atlas (TCGA) database. Then, seven miRNAs were found as important prognosis indicators of KIRC by Cox regression analysis and Lasso analysis. Subsequently, we established a seven miRNAs-clinical model to predict the prognosis of KIRC patients. The expressions of the 7 miRNAs between KIRC tissues and adjacent non-tumorous tissues were also examined.

2 | MATERIALS AND METHODS

2.1 | Data Processing

We downloaded the mature miRNA sequencing data of KIRC from the TCGA database, including 71 normal and 545 tumor tissues. Besides, the clinical information of KIRC patients was obtained. The patients with the survival time of 0 day were excluded. The clinical information table is

TABLE 1 Clinical characteristics of patients with KIRC from the TCGA database

Variables	TCGA set, n = 512
Death(%)	170 (33.20%)
Age(years)	57 ± 31
Gender(%)	
Female	178 (34.77%)
Male	334 (65.23%)
Grade(%)	
G1	12 (2.34%)
G2	217 (42.38%)
G3	201 (39.26%)
G4	74 (14.45%)
Missing	8 (1.56%)
Stage(%)	
Stage I	249 (48.63%)
Stage II	55 (10.74%)
Stage III	123 (24.02%)
Stage IV	82 (16.02%)
Missing	3 (0.59%)
T(%)	
T1	255 (49.80%)
T2	67 (13.09%)
T3	179 (34.96%)
T4	11 (2.15%)
M(%)	
M0	404 (78.91%)
M1	78 (15.23%)
Missing	30 (5.86%)
N(%)	
N0	227 (44.34%)
N1	17 (3.32%)
Missing	268 (52.34%)

shown in Table 1. In addition, the mRNA expression data were downloaded. The edgeR R package was employed to perform analysis to identify differentially expressed miRNAs (DEmiRNAs) and differentially expressed mRNAs (DEmRNAs).¹⁰ The DEmiRNAs and DE mRNAs were selected with the conditions: $|\log \text{fold change (FC)}| > 1.5$ and adjusted p value < 0.05 .

2.2 | miRNA model construction

Univariate Cox regression analysis was performed by using the survival R package and 24 DEmiRNAs related to prognosis were selected by setting $p < 0.01$. Lasso Cox regression was performed to remove miRNAs that were highly

overfitted.¹¹ Therefore, 14 miRNAs were chosen by LASSO Cox regression analysis. Finally, seven miRNAs were selected by multivariate Cox regression analysis and a risk score formula was constructed according to their coefficient. The formula was as follows: Risk score = $\sum \text{Coef miRNAs} * \log_2 (\text{Expression of miRNAs} + 1)$. Then, each patient's risk score was calculated based on the formula and all patients were divided into high- and low- risk groups according to the median score. In addition, we used the receiver operating characteristic (ROC) curve to evaluate the specificity and sensitivity of the prognostic miRNAs risk model by survivalROC R package.

2.3 | Functional enrichment analysis

In order to better understand the functional enrichment pathways of high- and low-risk groups, we performed gene set enrichment analysis (GSEA). The important pathways were picked out by NOM-*p* value < 0.05. Then, we predicted the target genes of these 7 miRNAs by website miRWalk and took the intersection with DE mRNAs.¹² Target DE mRNAs were submitted to the website DAVID to perform Gene Ontology (GO) and Kyoto Encyclopedia of Genes and Genomes (KEGG) enrichment analysis. The terms with *p* less than 0.05 were considered statistically significant.

2.4 | Clinical independence prognosis analysis for the risk model

To evaluate the independent prognostic ability of the risk model, both clinical features (age, gender, grade, stage, T, M, and N) and the 7-miRNA risk model were analyzed into the univariate and multivariate Cox regression analyses. The factors meeting *p* < 0.05 were considered statistically significant. The results of multivariate Cox analysis with *p* < 0.05 were considered as independent prognostic factors to predict the prognosis of KIRC.

2.5 | Construction of a miRNAs-clinical nomogram

The independent prognostic factors of KIRC were included in the miRNAs-clinical nomogram.¹³ The calibration curve analysis was utilized to evaluate the accuracy between the predicted and actual mortalities. The ROC and decision curve analysis (DCA) for the age, M, miRNA, and combined models (age, M, and miRNA model) were simultaneously analyzed.¹⁴ The clinical net benefit of the established nomogram was shown in the DCA.

2.6 | 7 miRNA expression levels between paired KIRC and adjacent non-tumorous tissues

A total of 20 paired KIRC and adjacent non-tumorous tissue samples were obtained from the First Affiliated Hospital of Wenzhou Medical University. The Ethics Committee of the First Affiliated Hospital of Wenzhou Medical University approved the use of clinical samples. The patients/participants provided their written informed consent to participate in this study. The expressions of miRNAs were measured by quantitative real-time PCR (qRT-PCR). The total RNA content of KIRC and adjacent non-tumorous tissue was extracted by TRIzol reagent. Then, miRNA was reverse transcribed into cDNA using ribo SCRIPTTM Reverse Transcription Kit with the volume of 10 μ L. The expression level of miRNA was calibrated by U6. Real-time PCR was performed by using SYBR Green Master Mix on the 7500 Fast quantitative PCR System (Applied Biosystems). The Ct value of each well was recorded and the relative quantification of the product was performed by using the $2^{-\Delta Ct}$ method. Differences between para-tumor and KIRC group were compared using a Student's *t*-test. *p*-value < 0.05 was considered statistically significant.

3 | RESULTS

3.1 | Identification of DE miRNAs and DE mRNAs in KIRC

Using the edgeR R package, we identified the DE miRNAs and DE mRNAs between KIRC and para-tumor kidney tissues from the TCGA database, with the adjusted *p* < 0.05 and $|\log_{2} \text{FC}| > 1.5$ as the thresholds. There were 94 DE miRNAs (50 up and 44 downregulated) and 3646 DE mRNAs (2492 up and 1154 downregulated) in KIRC. The distributions of the DE miRNAs and DE mRNAs were shown in the volcano plots (Figure 1A,C). In addition, the expression profiles of DE miRNAs and DE mRNAs in KIRC were shown in the heat maps (Figure 1B,D).

3.2 | Identification and selection of significant miRNAs

Next, we investigated the correlation between DE miRNAs and KIRC survival, and 4 patients with the survival time of 0 day were excluded from 516 patients. Univariate Cox regression analysis was performed in 94 DE miRNAs. Then, a total of 24 prognostic-related miRNAs were found (*p* < 0.01, Table S1). Moreover, the Lasso Cox regression was applied to punish every variable to screen variables. Fourteen miRNAs

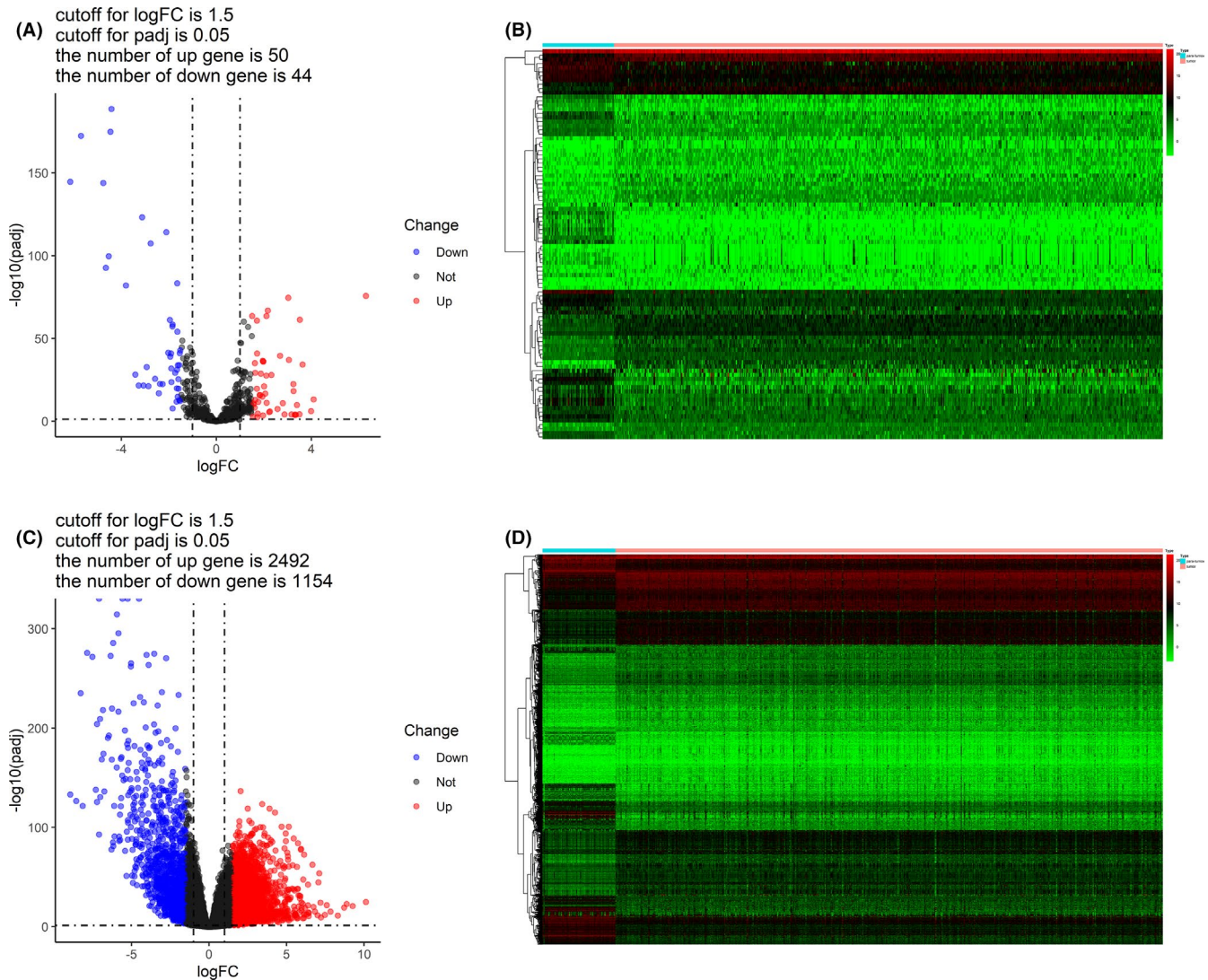


FIGURE 1 Differentially expressed miRNAs and mRNAs. (A) Volcano plot of differentially expressed miRNAs. (B) Heat map of differentially expressed miRNAs. (C) Volcano plot of differentially expressed mRNAs. (D) Heat map of differentially expressed mRNAs

were picked out by Lasso according to the minimal λ value (Figure S1). Finally, seven significant KIRC prognosis-related miRNAs (hsa-miR-21-5p, hsa-miR-3613-5p, hsa-miR-144-5p, hsa-miR-376a-5p, hsa-miR-5588-3p, hsa-miR-1269a, and hsa-miR-137-3p) were chosen by the multivariate Cox regression analysis. We next constructed a risk score formula based on the expression and cox coefficient of the seven miRNAs to predict the prognosis of KIRC:

$$\text{Risk score} = (0.4998 * \text{hsa-miR-21-5p}) + (0.5166 * \text{hsa-miR-3613-5p}) + (-0.2193 * \text{hsa-miR-144-5p}) + (0.1695 * \text{hsa-miR-376a-5p}) + (-0.1451 * \text{hsa-miR-5588-3p}) + (0.0550 * \text{hsa-miR-1269a}) + (0.1615 * \text{hsa-miR-137-3p}).$$

In this formula, the expressions of miRNAs were taken the log₂ value. Then, the risk scores of each patient were calculated by the risk formula. The patients were divided into high- and low-risk groups according to the median score. The results of

the risk score distribution, survival status, and miRNA expression showed that patients in the high-risk group had a higher probability of death than those with low risk (Figure 2A). The Kaplan–Meier curve indicated that patients in the low-risk group had better outcomes than those in the high-risk group ($p < 0.01$) (Figure 2B). The 1-, 3-, and 5-year survival probability of the high-risk group was 84.0%, 64.4%, and 47.6%. The 1-, 3-, and 5-year survival probability of the low-risk group was 95.5%, 86.6%, and 79.4%. Our data suggest that patients in the low-risk group have a longer survival time. Moreover, the ROC curve was used to evaluate the accuracy of the 7-miRNA model (Figure 2C). Notably, the area under the ROC curve (AUC) of the above model was 0.744. Besides, we examined the relation between risk scores and clinical features. There was no relation between age and risk scores (Figure 3A). Compared with female patients, higher risk scores were found in male patients (Figure 3B). The risk scores were increased along with higher level of grade, stage T, M, and N (Figure 3C–G). GSEA

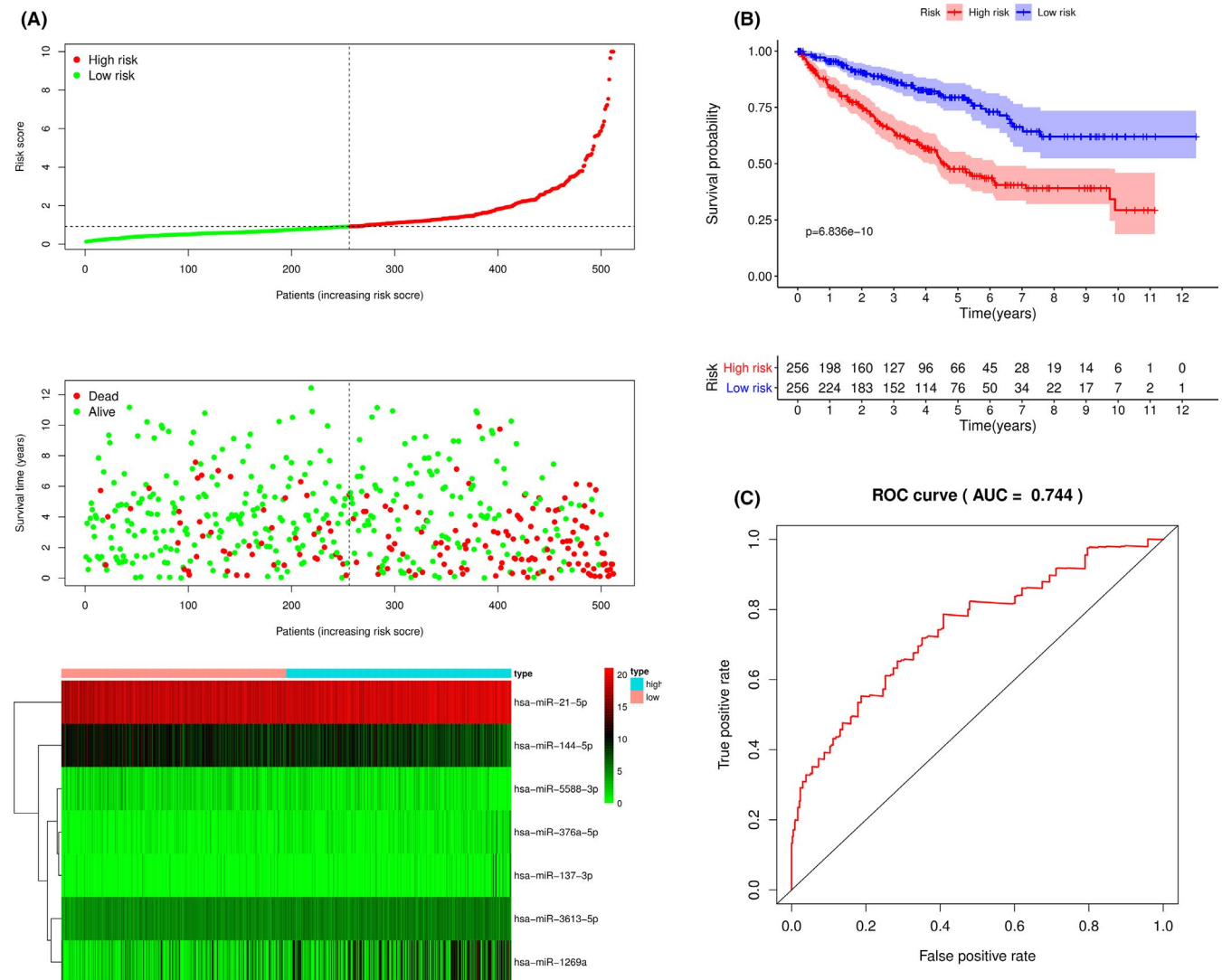


FIGURE 2 The 7-miRNA signature associated with overall survival of KIRC. (A) The upper panel represents risk score distribution for each patient, the middle panel shows the patient distribution with increasing risk value, and the lower panel represents the expressions of 7 prognostic miRNAs. (B) Kaplan-Meier curve analysis for the patients in KIRC between the high- and low-risk group. (C) ROC curve analysis for the 7-miRNA model for 1 year

analysis was performed to explore the potential pathways between the high- and low-risk groups. The results of GSEA indicated that several pathways including the DNA replication, P53 signaling pathway, adipocytokine signaling pathway, fatty acid metabolism, mTOR signaling pathway, PPAR signaling pathway, ErbB signaling pathway, and insulin signaling pathway, may be involved in the progression of KIRC (Figure S2).

3.3 | GO and KEGG enrichment analysis for 7-miRNA target genes

To explore the downstream mechanisms of the seven miRNAs, the potential target genes were predicted via miRWalk. Then, we set the binding score as 1 and took the intersection of predicted genes with DEMRNAs. Subsequently, 675

target genes were selected. To determine the roles of the 7-miRNA in KIRC, we analyzed the enrichment functions of these selecting target genes by DAVID. We visualized the top 10 terms under the condition of $p < 0.05$. It was found that biological process (BP), the terms of cell adhesion, cell surface receptor signaling pathway, regulation of immune response, potassium ion transmembrane transport, potassium ion transport, and positive regulation of branching involved in ureteric bud morphogenesis may be associated with KIRC progression (Figure 4A). As indicated by Figure 4B, the cellular component (CC) of target genes was significantly enriched in both plasma membrane and ion channel of renal cells surface. In addition, the molecular function (MF) of the target genes is correlated with calcium ion binding, voltage-gated potassium channel activity, voltage-gated potassium channel activity, and inward rectifier potassium channel activity

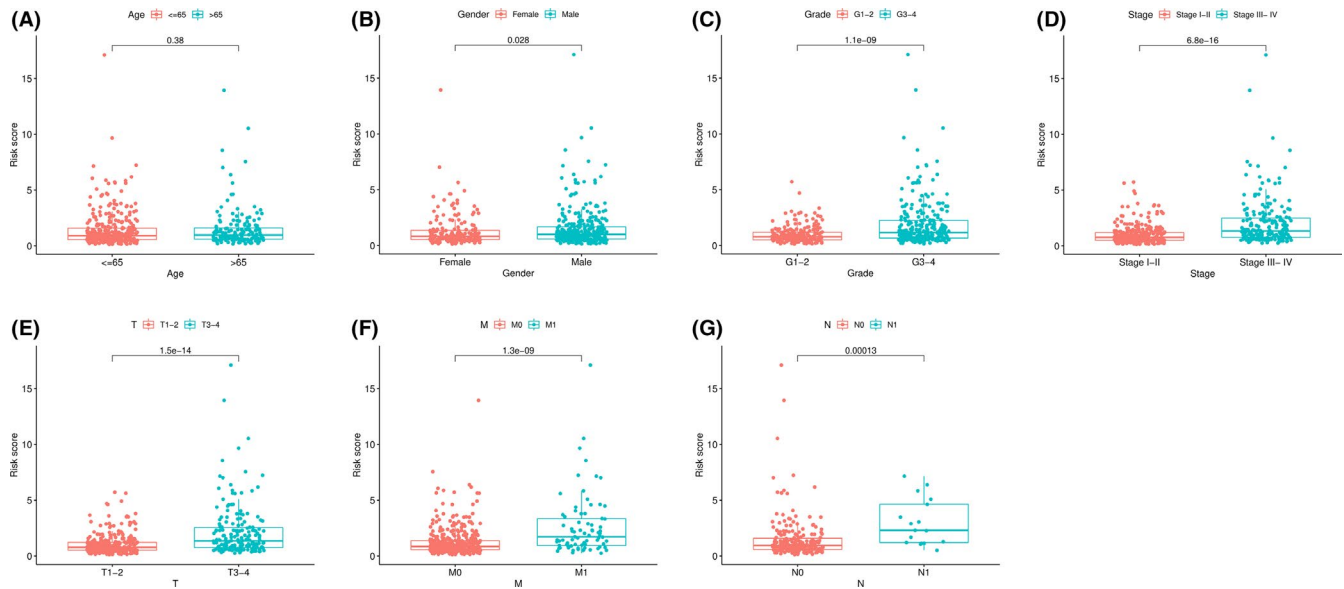


FIGURE 3 The correlation between risk scores and clinical features. Distribution of risk scores stratified by age (A), gender (B), grade (C), stage (D), T (E), M (F), and N (G)

(Figure 4C). The above target genes were also found to be involved in transcriptional misregulation in cancer, Ras signaling pathway, Rap1 signaling pathway, PI3K-Akt signaling pathway, Hippo signaling pathway, and calcium signaling pathway pathways, as shown by KEGG results (Figure 4D).

3.4 | Independent prognostic role of the miRNA signature

Both univariate and multivariate Cox regression analyses were performed to explore the independent prognostic ability of the 7-miRNA model with the clinical information including age, gender, grade, stage, T, M, and N. Univariate Cox analysis revealed that age ($p < 0.001$), grade ($p < 0.001$), stage ($p < 0.001$), T ($p < 0.001$), M ($p < 0.001$), N ($p < 0.001$), and miRNAs model risk score ($p < 0.001$) were significant risk factors associated with the prognosis of KIRC (Figure 5A). Multivariate Cox regression analysis demonstrated that age ($p < 0.001$), M ($p = 0.027$), and miRNA signature risk score ($p < 0.001$) may be the independent prognostic factors (Figure 5B).

3.5 | Stratified survival analysis

We also explored the accuracy of survival prediction in both high- and low-risk groups with clinical features. As shown in Figure 6, patients with low risk had a better survival probability than those with high risk in most clinical sub-groups. However, no significant results were found in the N1 subgroup due to the relatively low sample size.

3.6 | A nomogram with 7-miRNA model and clinical features

To determine the evaluation of miRNAs prognostic model and clinical features in the prognosis of KIRC patients, we built a nomogram that combined the miRNAs prognostic model with the clinical features such as age and metastasis (Figure 7). Moreover, the calibration plots of this nomogram for 1, 3, and 5 years are shown in Figure S3A–C. All the blue full lines were near to the broken line, suggesting that the combined model had a good performance in predicting the prognosis of KIRC. The AUC values for age, metastasis, and miRNAs prognostic model were additionally evaluated. As shown in Figure 8A–C, the AUC values for 1-, 3-, and 5-year overall survival (OS) were 0.657, 0.588, and 0.611 in age, 0.716, 0.660, and 0.629 in metastasis, and 0.747, 0.740, and 0.737 in the miRNAs prognostic model, respectively. Interestingly, the AUC values were obviously increased in the combined model. Furthermore, DCA was used to evaluate the efficiency of this nomogram. As shown in Figure 8D–F, our miRNAs model with clinical factors showed a better net benefit in predicting OS.

3.7 | Verification of seven miRNAs expression levels between paired KIRC and adjacent non-tumorous tissues

To verify the expressions of the seven miRNAs, qRT-PCR was performed in para-tumor tissues as well as in KIRC tissues. The results of qRT-PCR revealed that six prognostic miRNAs were highly expressed in KIRC tissues while hsa-miR-376a-5p was reduced (Figure 9).

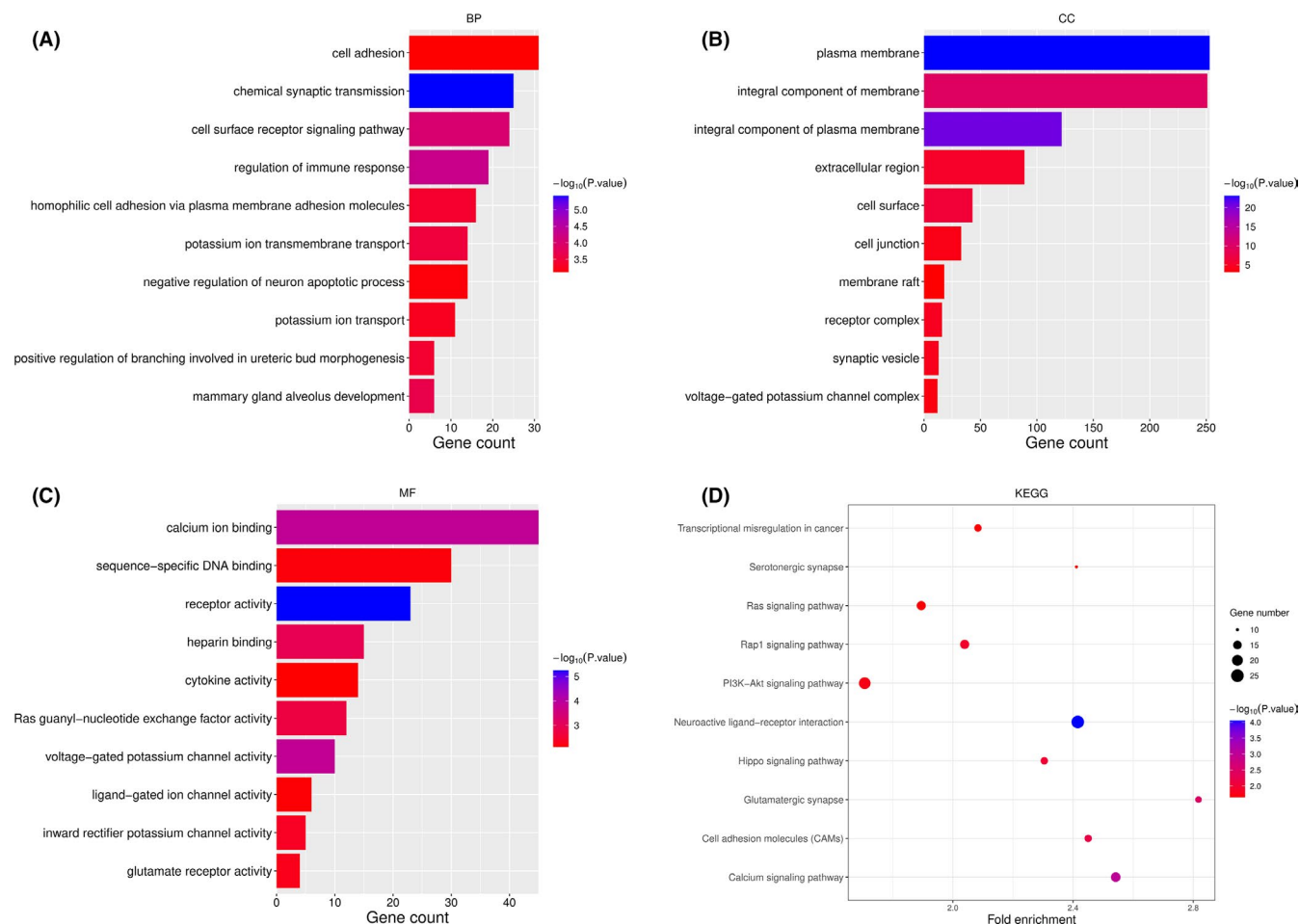


FIGURE 4 GO and KEGG enrichment analysis of target genes for 7 significant miRNAs. (A) Biological Process (BP). (B) Cellular Component (CC). (C) Molecular Function (MF). (D) KEGG

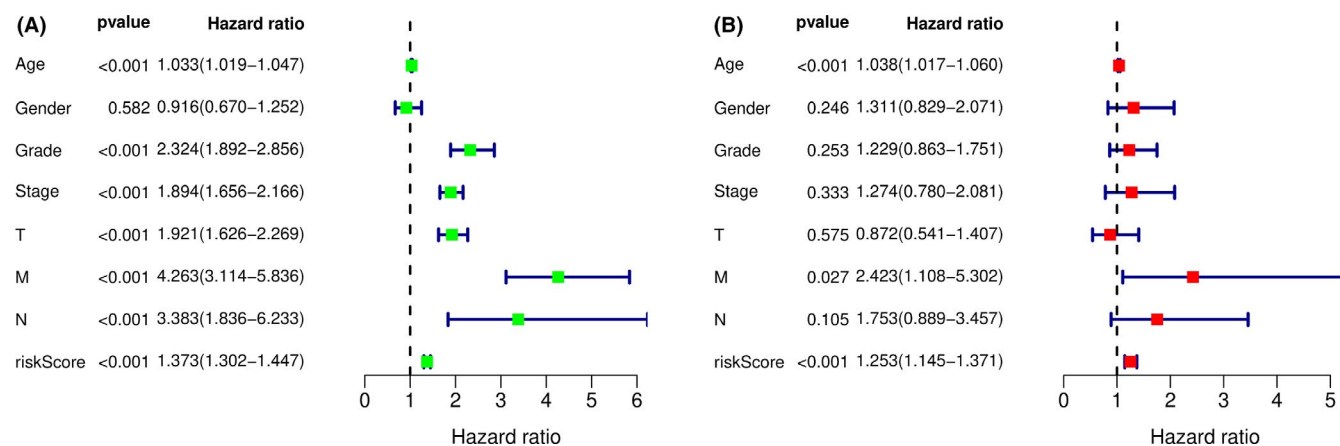


FIGURE 5 Independent prognosis analysis between clinical features and 7-miRNA prognostic model. (A) Univariate Cox regression analysis between clinical features and 7-miRNA prognostic risk score. (B) Multivariate Cox regression analysis between clinical features and 7-miRNA prognostic risk score

4 | DISCUSSION

Clear cell renal cell carcinoma (ccRCC) is a kind of solid tumor originating in renal tubules and insensitive to radiotherapy and chemotherapy.^{15,16} It has been reported that the disorders

of miRNAs may be involved in many diseases.¹⁷ With the development of technology, miRNAs have been demonstrated to be dysregulated in KIRC patients.¹⁸ Currently, there are few miRNAs-clinical models for predicting the prognosis of KIRC. Herein, a new miRNAs-clinical model was constructed

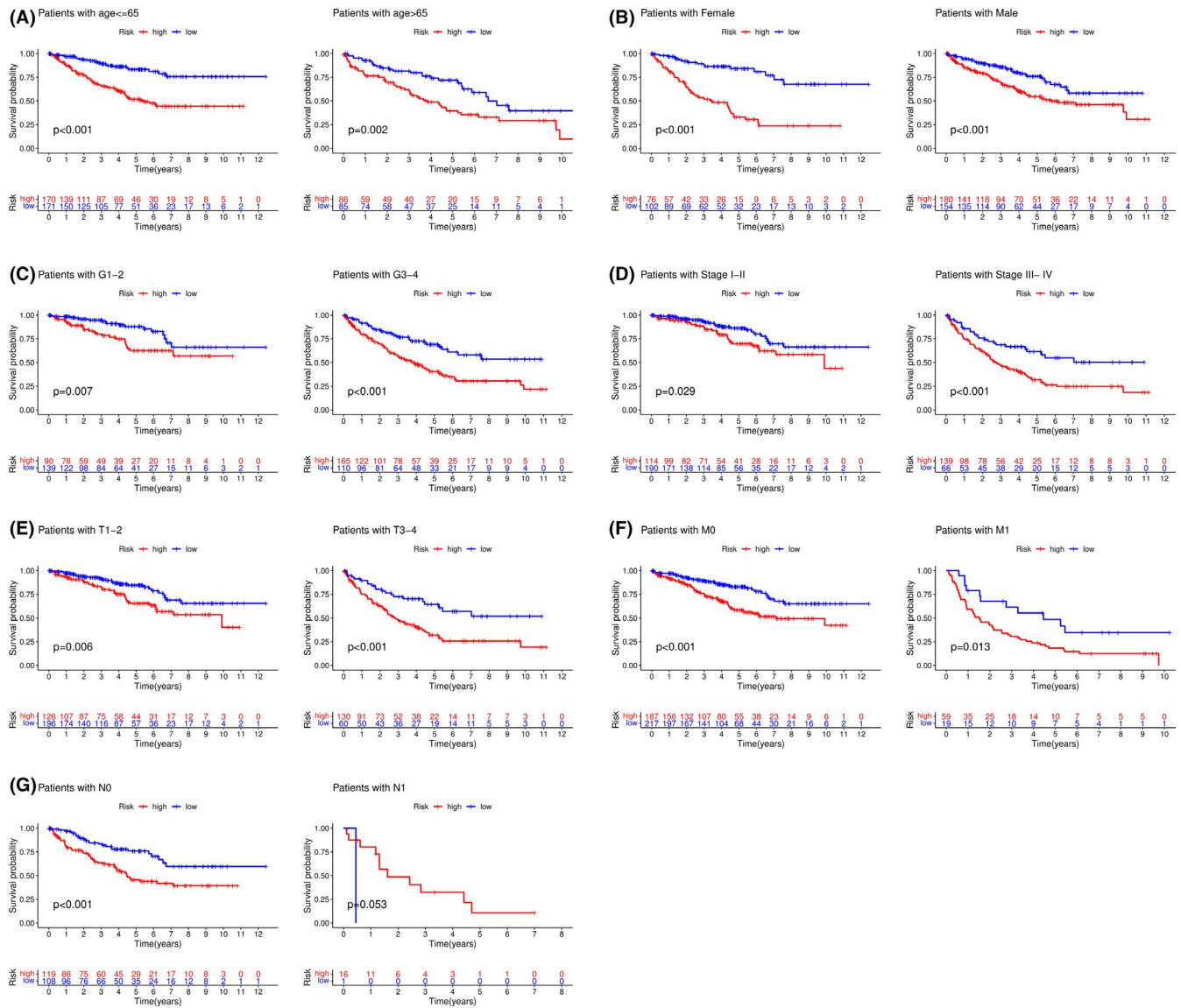


FIGURE 6 Survival analysis of all high- and low-risk group patients stratified by clinical features. Kaplan-Meier curves for patients in different level groups of age (A), gender (B), grade (C), stage (D), T (E), M (F), and N (G)

and used to evaluate the prognosis of KIRC patients. We systematically explored the prognosis and function of significant miRNAs in KIRC. Clearly, 94 DEMiRNAs were identified in KIRC patients based on TCGA data. Subsequently, a 7-miRNA signature was found and constructed, contributing to a better survival prediction in KIRC. Our findings may provide novel therapeutic targets for KIRC.

Hsa-miR-21-5p, hsa-miR-3613-5p, hsa-miR-144-5p, hsa-miR-376a-5p, hsa-miR-5588-3p, hsa-miR-1269a, and hsa-miR-137-3p were included in the 7-miRNA model. MiR-21 is an oncogenic miRNA that is upregulated in a variety of solid tumors. It has been reported that miR-21-5p promotes lung adenocarcinoma cell proliferation, migration, and invasion through targeting WWC2.¹⁹ Moreover, an increasing number of evidence has reported the involvement of miR-21-5p in KIRC prognosis.^{20,21} MiR-3613-5p has been reported to

be related to the metastasis of pancreatic cancer by targeting CDK6.²² Lu et al. have discovered that circRACGAP1 accelerates the progression of non-small cell lung cancer by miR-144-5p/CDKL1 signaling.²³ MiR-1269a has been found to be associated with the occurrence and process of hepatocellular carcinoma by targeting oncogenes SPATS2L and LRP6.²⁴ Previously, a 8-miRNA KIRC model has been constructed by Qin et al.²⁵ Interestingly, hsa-miR-3613-5p, hsa-miR-144-5p, and hsa-miR-1269a, which were incorporated in our model, were also found by them. MiR-137-3p, identified as a potential therapeutic target, suppresses the progression and metastasis of colorectal cancer cells by mediating the KDM1A-dependent epithelial-mesenchymal transition.²⁶ The roles of miR-376a-5p and miR-5588-3p have not been studied in cancers until now. Currently, the biological roles of seven miRNAs have been seldom explored in KIRC. Therefore,

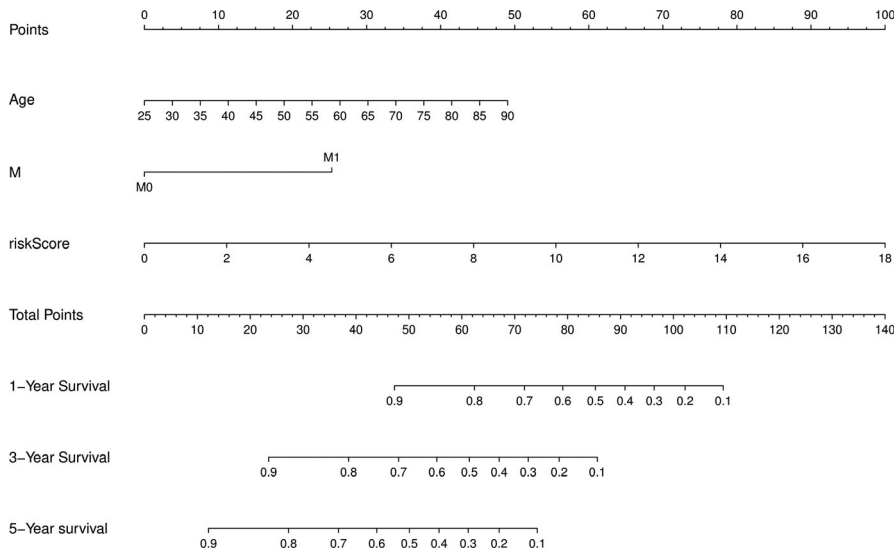


FIGURE 7 The miRNA-clinical nomogram to predict the survival probability of KIRC

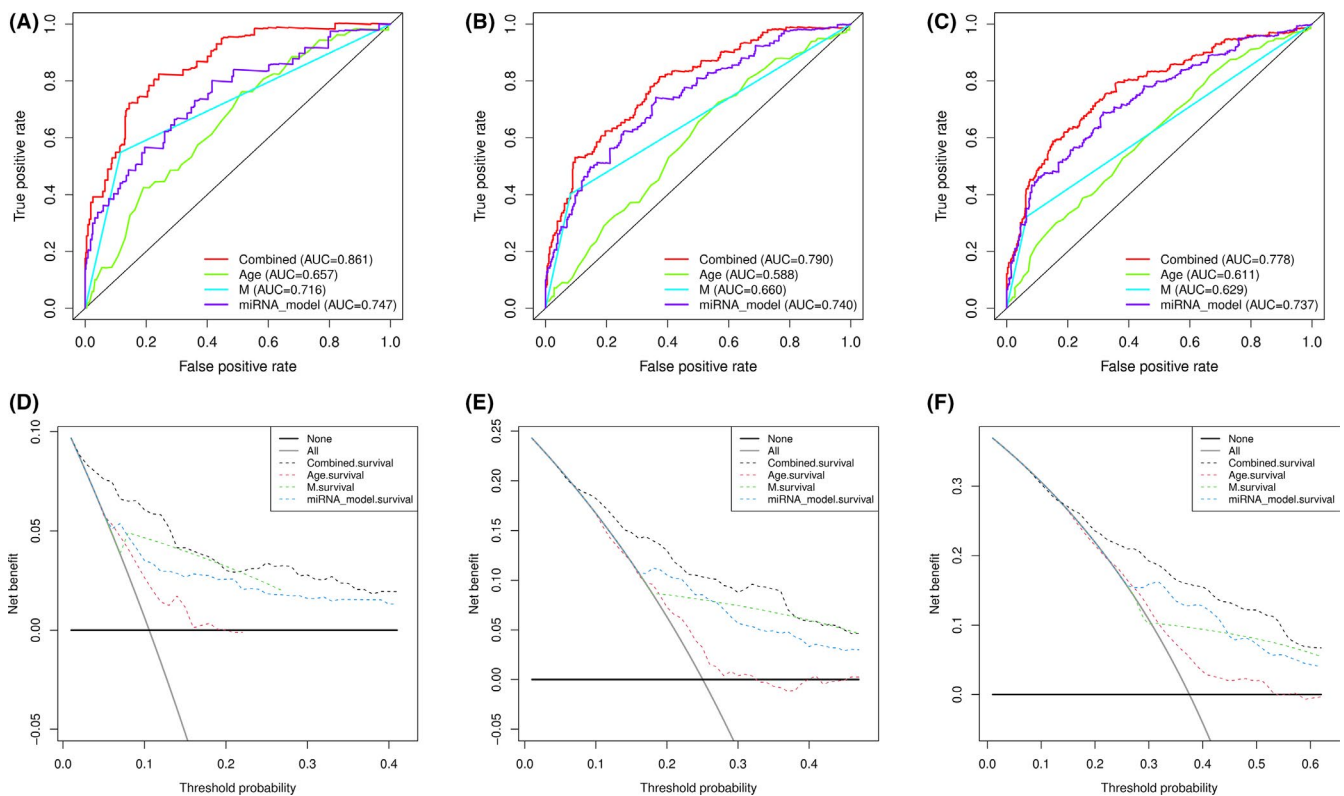


FIGURE 8 The ROC curve and DCA curve analysis to evaluate the accuracy of the nomogram at 1, 3 and 5 years, respectively. (A–C) ROC curve analysis of the nomogram compared for 1, 3, and 5 years. (D–F) DCA curve analysis of the nomogram compared for 1, 3, and 5 years

the exact contributions of these miRNAs in KIRC need to be further investigated. In this study, a risk model with the 7 miRNAs was built. In this model, the Kaplan–Meier curve showed that the low-risk group had a better survival rate. The ROC analysis revealed that this risk model contributed to the prediction of the prognosis of KIRC patients.

The GSEA results revealed many potential pathways for the miRNA model, among which adipocytokine signaling pathway, fatty acid metabolism, mTOR signaling pathway,

PPAR signaling pathway, ErbB signaling pathway, and insulin signaling pathway were enriched in the low-risk group. It is known that obesity has been considered an important dangerous factor for KIRC.²⁷ Therefore, the adipocytokine signaling pathway and fatty acid metabolism may be involved in KIRC progression. Increasing evidence have shown that the mTOR signaling pathway,²⁸ PPAR signaling pathway,²⁹ ErbB signaling pathway,³⁰ and insulin signaling pathway³¹ are significant cancer-related pathways. Moreover, it has

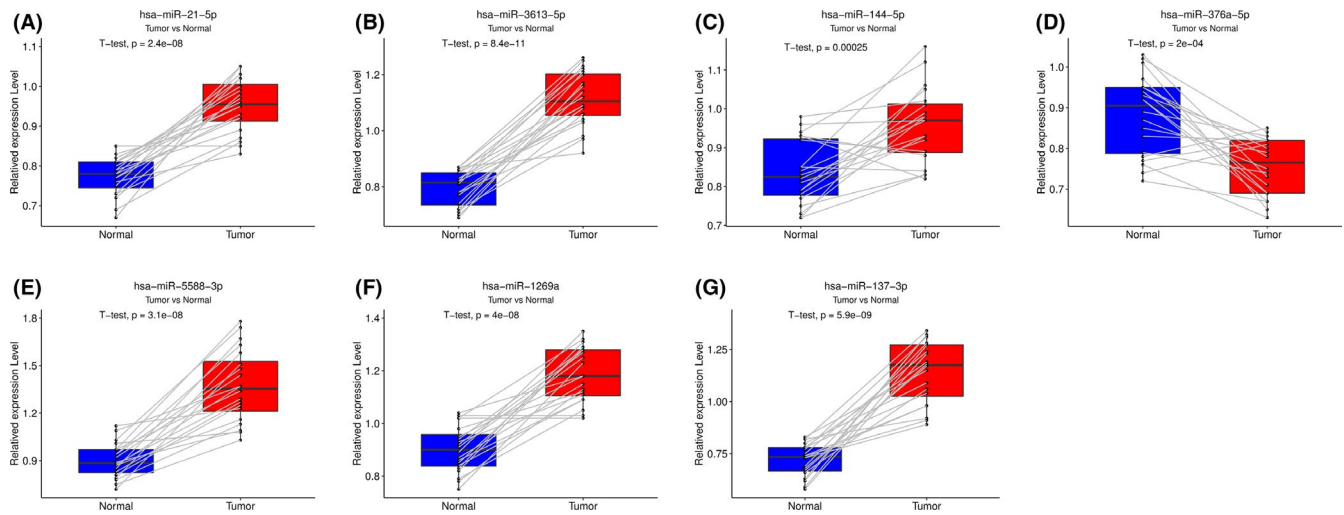


FIGURE 9 Experimental validation of 7 miRNAs between para-tumor and KIRC tissue by qRT-PCR. (A) hsa-miR-21-5p, (B) hsa-miR-3613-5p, (C) hsa-miR-144-5p, (D) hsa-miR-376a-5p, (E) hsa-miR-5588-3p, (F) hsa-miR-1269a, and (G) hsa-miR-137-3p

been found that DNA replication and P53 signaling pathway, highly correlated with the genesis and development of tumors, were enriched in high-risk group.^{32,33} Taken together, our results reveal the molecular regulatory network of the new model.

Next, the target genes of the seven miRNAs were predicted, which were performed in enrichment analysis. GO analysis indicated that the target genes were enriched in potassium ion transmembrane transport, potassium ion transport, and positive regulation of branching involved in ureteric bud morphogenesis, which was consistent with the previous studies in KIRC.^{34,35} The results of KEGG revealed that the target genes were mainly enriched in transcriptional misregulation in cancer, Ras signaling pathway, Rap1 signaling pathway, PI3K-Akt signaling pathway, Hippo signaling pathway, and calcium signaling pathway pathways. In fact, transcription regulation, Ras signaling pathway,³⁶ Rap1 signaling pathway,³⁷ PI3K-Akt signaling pathway,³⁸ Hippo signaling pathway,^{39,40} and calcium signaling pathway pathways⁴¹ are involved in the occurrence and development of various cancers. Combined with these, our results not only suggest the association of the seven miRNAs with tumorigenesis and progression of KIRC, but also provide the potential pathways of these miRNAs in the treatment of KIRC.

The inclusion of clinical factors into the genetic model contributes to the improvement of the accuracy of the prediction model. In this study, a nomogram, which integrated the 7-miRNA signature and two clinical independent risk factors to predict the prognosis of KIRC, was established. Notably, the miRNAs-clinical nomogram had a good ability in predicting the prognosis of KIRC.

In fact, few prognostic miRNA models have been established in KIRC. In comparison with the previous models, more statistical methods were used to obtain prognostic miRNAs in our model. In addition, clinical features were

integrated into this miRNA model in KIRC to build a nomogram, and this is the first report. Furthermore, the expressions of seven miRNAs were examined in KIRC tissues, which should be confirmed in the studies with larger sample sizes. In the future, more clinical databases should be used to verify the accuracy of the 7-miRNA model.

In conclusion, we disclose a novel miRNA-clinical prognosis model for KIRC, contributing to the evaluation of KIRC prognosis.

ACKNOWLEDGMENTS

The project was supported by the National Natural Science Foundation of China (No. 81873576), the Medical Health Science and Technology Project of Zhejiang Provincial Health Commission (No.2020RC081), and the project of Wenzhou Medical University Basic Scientific Research (No. KYYW201904).

CONFLICT OF INTEREST

The authors confirm that there are no conflicts of interest.

ETHICS APPROVAL

The studies involving human participants were reviewed and approved by the Human Research Ethics Committee in The First Affiliated Hospital of Wenzhou Medical University. The patients/participants provided their written informed consent to participate in this study. Written informed consent was obtained from the individual(s) for the publication of any potentially identifiable images or data included in this article.

DATA AVAILABILITY STATEMENT

Publicly available datasets were analyzed in this study. This data can be found here: <http://protal.gdc.cancer.gov>, <http://mirwalk.umm.uni-heidelberg.de/>, and <https://david.ncifcrf.gov/>.

ORCID

Yong Guo  <https://orcid.org/0000-0001-5881-112X>

REFERENCES

- Gray RE, Harris GT. Renal cell carcinoma: diagnosis and management. *Am Fam Physician*. 2019;99(3):179-184.
- Shingarev R, Jaimes EA. Renal cell carcinoma: new insights and challenges for a clinician scientist. *Am J Physiol Renal Physiol*. 2017;313(2):F145-F154.
- Zhao E, Li L, Zhang W, et al. Comprehensive characterization of immune- and inflammation-associated biomarkers based on multi-omics integration in kidney renal clear cell carcinoma. *J Transl Med*. 2019;17(1):177.
- Yin L, Li W, Wang G, et al. NR1B2 suppress kidney renal clear cell carcinoma (KIRC) progression by regulation of LATS 1/2-YAP signaling. *J Exp Clin Cancer Res*. 2019;38(1):343.
- Hsieh JJ, Purdue MP, Signoretti S, et al. Renal cell carcinoma. *Nat Rev Dis Primers*. 2017;3:17009.
- O'Brien J, Hayder H, Zayed Y, Peng C. Overview of MicroRNA biogenesis, mechanisms of actions, and circulation. *Front Endocrinol (Lausanne)*. 2018;9:402.
- Ali Syeda Z, Langden SSS, Munkhzul C, Lee M, Song SJ. Regulatory mechanism of MicroRNA expression in cancer. *Int J Mol Sci*. 2020;21(5):1723.
- Fan B, Jin Y, Zhang H, et al. MicroRNA21 contributes to renal cell carcinoma cell invasiveness and angiogenesis via the PDCD4/cJun (AP1) signalling pathway. *Int J Oncol*. 2020;56(1):178-192.
- Feng J, Guo Y, Li Y, et al. Tumor promoting effects of circRNA_001287 on renal cell carcinoma through miR-144-targeted CEP55. *J Exp Clin Cancer Res*. 2020;39(1):269.
- Nikolayeva O, Robinson MD. edgeR for differential RNA-seq and ChIP-seq analysis: an application to stem cell biology. *Methods Mol Biol*. 2014;1150:45-79.
- Tibshirani R. The lasso method for variable selection in the Cox model. *Stat Med*. 1997;16(4):385-395.
- Dweep H, Sticht C, Pandey P, Gretz N. miRWalk—database: prediction of possible miRNA binding sites by "walking" the genes of three genomes. *J Biomed Inform*. 2011;44(5):839-847.
- Iasonos A, Schrag D, Raj GV, Panageas KS. How to build and interpret a nomogram for cancer prognosis. *J Clin Oncol*. 2008;26(8):1364-1370.
- Tsalatsanis A, Hozo I, Vickers A, Djulbegovic B. A regret theory approach to decision curve analysis: a novel method for eliciting decision makers' preferences and decision-making. *BMC Med Inform Decis Mak*. 2010;10:51.
- Andreiana BC, Stepan AE, Margaritescu C, et al. Histopathological prognostic factors in clear cell renal cell carcinoma. *Curr Health Sci J*. 2018;44(3):201-205.
- Sliwinska-Jewsiewicka A, Kowalczyk AE, Krazinski BE, et al. Decreased expression of SATB2 associates with tumor growth and predicts worse outcome in patients with clear cell renal cell carcinoma. *Anticancer Res*. 2018;38(2):839-846.
- Vishnoi A, Rani S. MiRNA biogenesis and regulation of diseases: an overview. *Methods Mol Biol*. 2017;1509:1-10.
- Braga EA, Fridman MV, Loginov VI, Dmitriev AA, Morozov SG. Molecular mechanisms in clear cell renal cell carcinoma: role of miRNAs and hypermethylated miRNA genes in crucial oncogenic pathways and processes. *Front Genet*. 2019;10:320.
- Wang G, Zhou Y, Chen W, et al. miR-21-5p promotes lung adenocarcinoma cell proliferation, migration and invasion via targeting WWC2. *Cancer Biomark*. 2020;28(4):549-559.
- Huang M, Zhang TI, Yao Z-Y, et al. MicroRNA related prognosis biomarkers from high throughput sequencing data of kidney renal clear cell carcinoma. *BMC Med Genomics*. 2021;14(1):72.
- Xie M, Lv Y, Liu Z, et al. Identification and validation of a four-miRNA (miRNA-21-5p, miRNA-9-5p, miR-149-5p, and miRNA-30b-5p) prognosis signature in clear cell renal cell carcinoma. *Cancer Manag Res*. 2018;10:5759-5766.
- Cao R, Wang K, Long M, et al. miR-3613-5p enhances the metastasis of pancreatic cancer by targeting CDK6. *Cell Cycle*. 2020;19(22):3086-3095.
- Lu M, Xiong H, Xia Z-K, et al. circRACGAP1 promotes non-small cell lung cancer proliferation by regulating miR-144-5p/CDKL1 signaling pathway. *Cancer Gene Ther*. 2021;28(3-4):197-211.
- Min P, Li W, Zeng D, et al. A single nucleotide variant in microRNA-1269a promotes the occurrence and process of hepatocellular carcinoma by targeting to oncogenes SPATS2L and LRP6. *Bull Cancer*. 2017;104(4):311-320.
- Qin S, Shi X, Wang C, Jin P, Ma F. Transcription factor and miRNA interplays can manifest the survival of ccRCC patients. *Cancers*. 2019;11(11).
- Ding X, Zhang J, Feng Z, Tang Q, Zhou X. MiR-137-3p inhibits colorectal cancer cell migration by regulating a KDM1A-dependent epithelial-mesenchymal transition. *Dig Dis Sci*. 2021;66(7):2272-2282.
- Kovesdy CP, Furth S, Zoccali C. World kidney day steering C. obesity and kidney disease: Hidden consequences of the epidemic. *Physiol Int*. 2017;104(1):1-14.
- Robb VA, Karbowniczek M, Klein-Szanto AJ, Henske EP. Activation of the mTOR signaling pathway in renal clear cell carcinoma. *J Urol*. 2007;177(1):346-352.
- Abu About O, Wettersten HI, Weiss RH. Inhibition of PPARalpha induces cell cycle arrest and apoptosis, and synergizes with glycolysis inhibition in kidney cancer cells. *PLoS One*. 2013;8(8):e71115.
- Dong W, Cao Z, Pang Y, Feng T, Tian H. CARF, as an oncogene, promotes colorectal cancer stemness by activating ERBB signaling pathway. *Oncotargets Ther*. 2019;12:9041-9051.
- Li Z-H, Xiong Q-Y, Xu L, et al. miR-29a regulated ER-positive breast cancer cell growth and invasion and is involved in the insulin signaling pathway. *Oncotarget*. 2017;8(20):32566-32575.
- Huang J. Current developments of targeting the p53 signaling pathway for cancer treatment. *Pharmacol Ther*. 2021;220:107720.
- Kitao H, Iimori M, Kataoka Y, et al. DNA replication stress and cancer chemotherapy. *Cancer Sci*. 2018;109(2):264-271.
- Thoenes W, Störkel S, Rumpelt H. Histopathology and classification of renal cell tumors (adenomas, oncocytomas and carcinomas). The basic cytological and histopathological elements and their use for diagnostics. *Pathol Res Pract*. 1986;181(2):125-143.
- Wadhwa S, Wadhwa P, Dinda AK, Gupta NP. Differential expression of potassium ion channels in human renal cell carcinoma. *Int Urol Nephrol*. 2009;41(2):251-257.
- Adjei AA. Blocking oncogenic Ras signaling for cancer therapy. *J Natl Cancer Inst*. 2001;93(14):1062-1074.
- Kim WJ, Gersey Z, Daaka Y. Rap1GAP regulates renal cell carcinoma invasion. *Cancer Lett*. 2012;320(1):65-71.

38. Peng X-S, Yang J-P, Qiang Y-Y, et al. PTPN3 inhibits the growth and metastasis of clear cell renal cell carcinoma via inhibition of PI3K/AKT signaling. *Mol Cancer Res.* 2020;18(6):903-912.
39. Lv M, Li S, Luo C, et al. Angiotensin promotes renal epithelial and carcinoma cell proliferation by retaining the nuclear YAP. *Oncotarget.* 2016;7(11):12393-12403.
40. Yang W-H, Ding C-K, Sun T, et al. The hippo pathway effector TAZ regulates ferroptosis in renal cell carcinoma. *Cell Rep.* 2019;28(10):2501-2508.
41. Liu X, Yang Z, Luo X, et al. Calcium-activated nucleotidase 1 silencing inhibits proliferation, migration, and invasion in human clear cell renal cell carcinoma. *J Cell Physiol.* 2019;234(12):22635-22647.

SUPPORTING INFORMATION

Additional supporting information may be found online in the Supporting Information section.

How to cite this article: Zhan Y, Zhang R, Li C, et al. A microRNA-clinical prognosis model to predict the overall survival for kidney renal clear cell carcinoma. *Cancer Med.* 2021;10:6128–6139. <https://doi.org/10.1002/cam4.4148>